






Oxidized glutathione promotes association between eukaryotic translation elongation factor 1B γ and Ure2p glutathione transferase from *Phanerochaete chrysosporium*

Raphael Bchini , Jean-Michel Girardet , Rodney Sormani , Eric Gelhaye  and Mélanie Morel-Rouhier 

Université de Lorraine, Nancy, France

Keywords

eEF1B γ ; glutathione transferase; GSSG; time-resolved molecular dynamics

Correspondence

M. Morel-Rouhier, UMR 1136 INRAE-Université de Lorraine 'Interactions Arbres/Micro-organismes', BP 70239, F-54506 Vandœuvre-lès-Nancy Cedex, France
 Tel: +33 3 72 74 51 62
 E-mail: melanie.morel@univ-lorraine.fr

[Correction added on 29 November 2020, after first online publication: Peer review history is not available for this article, so the peer review history statement has been removed.]

(Received 5 June 2020, revised 10 September 2020, accepted 27 October 2020)

doi:10.1111/febs.15614

The eukaryotic translation elongation factor 1B γ (eEF1B γ) is an atypical member of the glutathione transferase (GST) superfamily. Contrary to more classical GSTs having a role in toxic compound detoxification, eEF1B γ is suggested to act as a scaffold protein, anchoring the elongation factor complex EF1B to the endoplasmic reticulum. In this study, we show that eEF1B γ from the basidiomycete *Phanerochaete chrysosporium* is fully active as a glutathione transferase *in vitro* and undergoes conformational changes upon binding of oxidized glutathione. Using real-time analyses of biomolecular interactions, we show that GSSG allows eEF1B γ to physically interact with other GSTs from the Ure2p class, opening new perspectives for a better understanding of the role of eEF1B γ in cellular oxidative stress response.

Introduction

The elongation factor eEF1B γ is a widespread protein in eukaryotic organisms. It is part of the eEF1B complex, also comprising eEF1B α , which acts as a guanine nucleotide exchange factor during the elongation step of protein translation. In *Saccharomyces cerevisiae*, this complex is composed of only two subunits (eEF1B γ and eEF1B α), while in human it involves two additional factors eEF1B β and eEF1B δ (also described as eEF1 β and eEF1 δ) [1,2]. While eEF1B α , eEF1B β , and eEF1B δ have sites for nucleotide exchange activity, eEF1B γ does not. The function of eEF1B γ within

the elongation complex is thus not well understood. eEF1B γ has been proposed to act in translation elongation as a structural scaffold for eEF1B α by helping the binding of the complex to the endoplasmic reticulum [3]. The eEF1B γ subunit could anchor at the membrane via its C terminus end and interact with the N terminus of eEF1B α , eEF1B β and/or eEF1B δ subunits [2,4].

Various other roles have been proposed for eEF1B γ in particular for the human isoform. For example, eEF1 γ functions as a positive regulator of NF- κ B

Abbreviations

CDNB, chlorodinitrobenzene; DTNB, 5,5'-Dithiobis(2-nitrobenzoic acid); eEF1B, eukaryotic elongation factor 1B; GSSG, oxidized glutathione; GST, glutathione transferase; ITC, isothermal titration calorimetry; NT-heEF1 γ , N terminus domain of human eEF1B γ .

signaling by targeting the mitochondrial antiviral-signaling protein for activation, which provides a new regulatory mechanism of antiviral responses [5]. eEF1B γ can also interact with cytoskeleton. In mouse, eEF1 γ depletion affects keratin synthesis and causes the Vimentin protein, to be incorrectly compartmentalized. Since, Vimentin is an intermediate filament protein important in the dynamic organization of the cytoskeleton, this severely compromises cellular shape and mitochondria localization [6]. Moreover, eEF1 γ depletion increases mitochondrial superoxide generation as well as the total levels of carbonylated proteins [7], providing evidence, that eEF1 γ is a key player in cellular stress responses. Accordingly, the level of eEF1B γ upregulation has been shown to positively correlate with tumor aggressiveness, presumably due to an altered redox balance [8–11].

In fungi, eEF1B γ has been poorly characterized and most of the studies focused on the *S. cerevisiae* isoform. In yeast, eEF1B γ is encoded by TEF3 and TEF4. They are nonessential genes, the products of which probably serve as positive regulators of the catalytic eEF1B α subunit [12]. Yeast strains lacking eEF1B γ display increased resistance to cadmium-induced stress but are deficient in vacuolar-dependent turnover of oxidized proteins [13,14].

The role of eEF1B γ in oxidative stress response could be linked to its glutathione transferase (GST) properties. The GST superfamily is ubiquitous in all living organisms. The major recognized role of GSTs is the detoxification of toxic substances by conjugating them with glutathione. In recent years, the accumulation of functional analyses concerning these proteins from organisms of various kingdoms such as human, bacteria, insects, plants, and fungi revealed several additional roles for GSTs. They can attenuate cell oxidative stress through glutathione peroxidase activities that play a crucial role in detoxifying lipid hydroperoxides [15]. In human, it has become obvious that GSTs are involved in the control of apoptosis through the inhibition of the c-Jun-N-terminal kinase (JNK) signaling pathway [16]. Some GSTs can also possess ligandin properties and thus participate in the intracellular transport of anthocyanins in plants [17], the intracellular scavenging of toxic molecules in wood-degrading fungi [18], or arsenate detoxification in human [19]. They can also be involved in the storage and transport of lipophilic compounds such as bile acids, fatty acids, and certain drugs in the aqueous phase of the human cell [20,21].

Although phylogenetic and structural studies showed unambiguously that eEF1B γ is a member of the GST superfamily [10,22,23], only little evidence is

available concerning its activity as a GST. In this study, we show that eEF1B γ from the basidiomycete fungus *Phanerochaete chrysosporium* possesses glutathione transferase activity and a high affinity for oxidized glutathione. Using real-time analyses of biomolecular interactions, we show that GSSG allows eEF1B γ to physically interact with other GSTs from the Ure2p class. These results strongly support the hypothesis that, in addition to its role as a scaffold protein stabilizing the EF1B complex, eEF1B γ could also be involved in cellular oxidative stress response in eukaryotes.

Results and Discussion

Sequence comparison of eEF1B γ from *P. chrysosporium* with the previously characterized yeast and human isoforms

One sequence (ProtID 2934909) coding for eEF1B γ was identified in *P. chrysosporium* genome database (Mycocosm: <https://mycocosm.jgi.doe.gov/Phchr2/Phchr2.home.html>) using the *S. cerevisiae* isoforms TEF3 and TEF4 as templates (cut off 10^{-5}). TEF3 and TEF4 share only 64.5% identity. PcEF1B γ exhibits 35.5% and 40.2% identity with TEF3 and TEF4, respectively, and 37.0% with the human eEF1B γ (ProtID 4503481). Amino acid alignment of *S. cerevisiae* TEF3 and TEF4, *P. chrysosporium*, and human eEF1B γ confirms the organization of the proteins into two conserved N-terminal GST and C-terminal EF1B γ domains connected by a variable linker (Fig. 1). The Pro50 and Glu62 residues (*S. cerevisiae* TEF3 numbering) involved in glutathione stabilization are present in the *P. chrysosporium* sequence. PcEF1B γ possesses two cysteines that are not conserved in the other eEF1B γ .

Both full-length PcEF1B γ and PcEF1B γ _GST domain are dimeric and active as glutathione transferases

The recombinant full-length PcEF1B γ and the PcEF1B γ _GST domain (as identified in Fig. 1) were successfully produced in a bacterial heterologous system and purified. Mass spectrometry analysis in nonreducing conditions showed that both proteins were purified without any covalently bound glutathione (Table 1). Additionally, no noncovalently bound glutathione was copurified with the proteins since no free glutathione [neither GSSG (molecular mass of 612.63 Da) nor GSH (molecular mass of 307.32 Da)] was detected within the PcEF1B γ sample. The recombinant PcEF1B γ was thus purified free of glutathione.

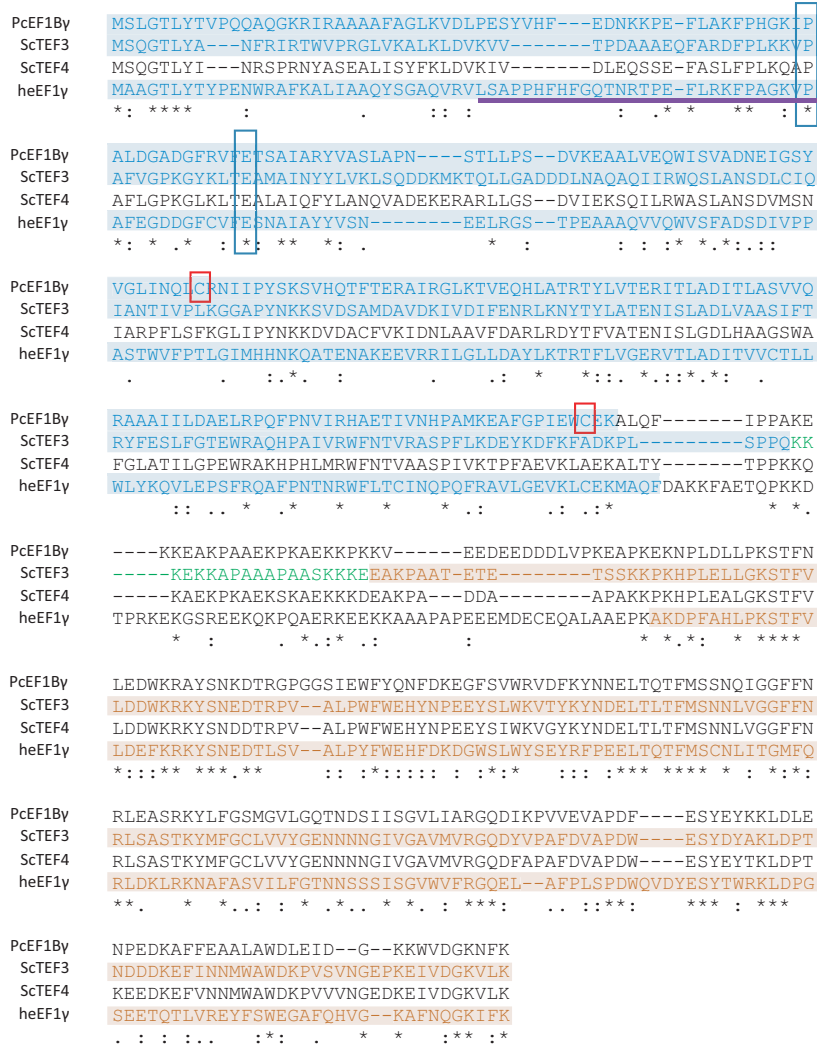


Fig. 1. Amino acid sequence alignment of eEF1B γ from *Phanerochaete chrysosporium* (PcEF1B γ), *Saccharomyces cerevisiae* (ScTEF3 and ScTEF4) and human (heEF1 γ). The GST and EF1B domains, as identified in previous studies [24,27], are labeled respectively in blue and orange. The part of PcEF1B γ which is in blue corresponds to the sequence of the recombinant PcEF1B γ _GST domain that has been produced and purified in this study. The portion in green corresponds to the linker that has been found required for the dimer stabilization of the GST domain of ScTEF3 [27]. The conserved Pro50 and Glu62 (*S. cerevisiae* TEF3 numbering) involved in glutathione binding are framed in blue, and the two cysteines of PcEF1B γ are framed in red. The sequence identified as being involved in the eEF1B β recognition loop is underlined in purple [27].

No GSSG was found in the PcEF1B γ _GST domain sample, and rather, trace amounts of GSH were detected.

Analyses by size exclusion chromatography with multi-angle light scattering (SEC-MALS) revealed that both PcEF1B γ and PcEF1B γ _GST domain were dimeric (Table 1). Accordingly, in human, both the full-length and the GST domain (defined as NT-heEF1 γ for N terminus domain of human eEF1B γ) form dimers [24]. Moreover, the NT-heEF1 γ , which may be responsible for the dimerization of the full protein due to its GST-fold, undergoes GSSG-induced dimerization [2]. No GSSG was detected in the dimer-forming PcEF1B γ _GST domain, but we cannot exclude a role of glutathione for PcEF1B γ _GST domain dimerization, because we have not obtained the PcEF1B γ _GST domain free of GSH. However, it

is unlikely that glutathione has a role in the dimer formation because the full-length PcEF1B γ dimer is free of glutathione. In *S. cerevisiae*, the dimerization of the GST domain is dependent on the presence of additional amino acids of the linker (see Fig. 1). This extension is not present in the sequence of PcEF1B γ _GST domain, suggesting that it is not needed for dimerization of the domain. This extension is also dispensable for the human GST domain dimerization [24].

Both full-length and GST domain of PcEF1B γ were active as glutathione transferases as demonstrated by their ability to transfer glutathione onto chlorodinitrobenzene (CDNB), which is the substrate commonly used for measuring GST activity (Table 2). The GST domain of PcEF1B γ exhibited better apparent affinities for both GSH and CDNB than the full-length

Table 1. Monomer and oligomer masses of PcEF1B γ and PcEF1B γ _GST domain determined by mass spectrometry (MS) and SEC-MALS, respectively.

	PcEF1B γ	PcEF1B γ _GST domain
Theoretical molecular mass (Da)	46 857.26 46 726.07 (–Met)	24 831.44 24 700.25 (–Met)
MS data (Da)	46 726.30 (–Met)	24 701.00 (–Met)
SEC-MALS data (Da)	98 710	48 460

protein, suggesting that the binding sites are more accessible for the substrate in absence of the C-terminal part of the protein. However, a better velocity was determined for the full-length PcEF1B γ . Taken together, these results showed similar catalytic efficiency for both proteins ($k_{\text{cat}}/K_M = 283$ and 248 for the full-length PcEF1B γ and the GST domain respectively), suggesting that the presence of the EFB domain has weak impact on the efficiency of the glutathionylation activity. As a comparison, k_{cat} of both isoforms is in the same range than those measured for other CDNB active GSTs of *P. chrysosporium* from the Ure2p class [25]. GST activity of recombinant eEF1B γ has only been reported for the *Oryza sativa* isoform after optimization of protein production to increase protein stability [26]. In human, no activity was measured for the full-length protein, while a weak one was measured for the GST domain (NT-heEF1 γ) [24]. In *S. cerevisiae*, only the GST domain has been produced [27]. It shows no GST activity even in the presence of the linker extension described above. In *Crithidia fasciculata*, while eEF1B γ is inactive as a purified recombinant protein, it displays GST activity when associated with the other subunits of the eEF1B complex [28]. This ability of eEF1B γ to transfer glutathione strongly suggests that in addition to having a role in the stabilization of the eEF1B complex, it could act as an active redox enzyme and thus be part of the cell response to oxidative stress.

PcEF1B γ efficiently binds GSSG leading to conformational changes of the protein

The interaction of PcEF1B γ or PcEF1B γ _GST domain with glutathione was investigated thermodynamically. The data showed a better affinity of the full-length protein for GSSG than for GSH ($K_d = 5.6$ and $19.2 \mu\text{M}$, respectively; Fig. 2 and Table 3). The PcEF1B γ _GST domain was also able to bind both

Table 2. Enzymatic activities of PcEF1B γ and PcEF1B γ _GST domain using chlorodinitrobenzene (CDNB). \pm SD ($n = 3$).

	K_m		k_{cat} (s^{-1})
	GSH (mM)	CDNB (mM)	
PcEF1B γ	1.27 ± 0.50	7.78 ± 1.18	2.20 ± 0.15
PcEF1B γ _GST domain	0.24 ± 0.05	1.61 ± 0.17	0.40 ± 0.01

GSSG and GSH, but with a slightly lower affinity compared to the full-length protein ($K_d = 14.9$ and $32.8 \mu\text{M}$, respectively). The stoichiometry of the interaction corresponded to one GSSG or GSH molecule bound per dimer of PcEF1B γ or PcEF1B γ _GST domain. Regarding the thermodynamic features, all of the four types of interactions dissipated similar energy in the form of work and progressed spontaneously (similar $\Delta G < 0$). The reactions were exothermic, and the glutathione binding was dominated by a large favorable enthalpy ($\Delta H \ll 0$) and an unfavorable binding entropy ($-\Delta S \gg 0$), with hydrophilic bonds involved, such as van der Waals and hydrogen bonds.

In human, eEF1 γ is able to bind GSH, GSSG, S-hexylglutathione, and glutathione sulfonate, as shown by isothermal titration calorimetry (ITC) thermodynamic approaches [29]. The Gibbs' free energies of the different interactions ($\Delta G = ca. -5.6 \text{ kcal}\cdot\text{mol}^{-1}$; [29]) are similar to those determined for PcEF1B γ (Table 3). However, contrary to PcEF1B γ , the human protein has slightly lower affinities for GSH than for GSSG (K_d of 67 and $115 \mu\text{M}$, respectively; [29]) (Table 3). The preference for GSH over GSSG by the full-length heEF1 γ could indicate that the C-terminal part may structurally influence glutathione binding to heEF1 γ by hindering the binding of GSSG [29]. Our data showed that this was not the case for PcEF1B γ , which preferentially bound GSSG over GSH, even more efficiently than the PcEF1B γ _GST domain devoid of the C-terminal part.

The sequence of PcEF1B γ contains two cysteines (Fig. 1). To check the redox state of the purified PcEF1B γ , alkylation tests with 2-kDa mPEG-maleimide were performed. The migration pattern on SDS/PAGE gel revealed that alkylation resulted in an increase of the size of the protein by 4 kDa, suggesting that both cysteines were reduced (Fig. 3A). This is in accordance with the mass spectrometry data, and it was confirmed by DTNB-based thiol titration (data not shown). Incubation of PcEF1B γ with glutathione (GSH, GSSG, or GSNO) prevented the binding of the alkylating agent, suggesting that thiols of both

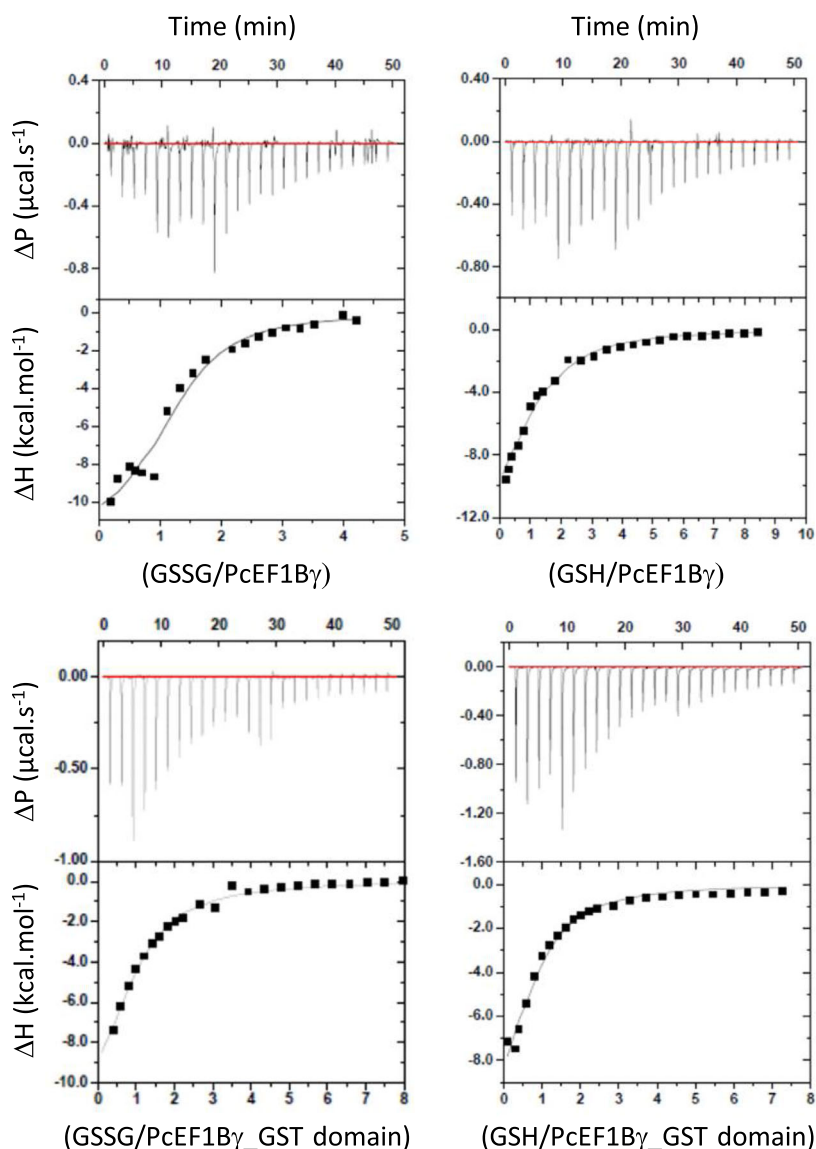


Fig. 2. Raw ITC data (bottom panels) and binding isotherms (top panels) for PcEF1B γ and PcEF1B γ _GST domain titrated either with GSSG or GSH. The solid line represents the results of nonlinear least-square fitting of the experimental data using the single-site model. The experiment has been performed in duplicates with independent protein preparations.

Table 3. Thermodynamics parameters of glutathione (GSH or GSSG) binding to PcEF1B γ or to PcEF1B γ _GST domain. The values were obtained by fitting the ITC data to a one-binding-site mode with ORIGIN software (N = number of binding sites per dimer, K_a = affinity constant, K_d = dissociation constant ($1/K_a$), ΔH = change in enthalpy, $-\Delta S$ = change in entropy, ΔG = Gibb's free energy). The standard variation, if any, is given in brackets. Each measurement was performed twice.

Sample	N	K_a (10^4 M $^{-1}$)	K_d (μ M)	ΔH (kcal·mol $^{-1}$)	$-\Delta S$ (kcal·mol $^{-1}$)	ΔG (kcal·mol $^{-1}$)
PcEF1B γ + GSH	1.06 (0.16)	5.21 (1.51)	20.9 (6.1)	-16.24 (3.23)	9.81	-6.43
PcEF1B γ + GSSG	1.23 (0.10)	17.90 (6.53)	6.4 (2.3)	-12.03 (1.30)	4.86	-7.14
PcEF1B γ _GST domain + GSH	0.98 (0.22)	3.05 (0.73)	33.4 (9.7)	-11.97 (3.36)	5.84	-6.13
PcEF1B γ _GST domain + GSSG	0.90 (0.10)	6.73 (1.13)	15.3 (2.6)	-14.43 (2.10)	7.93	-6.50

cysteines were not accessible anymore. A step of dialysis of PcEF1B γ after incubation with glutathione allowed restoring the binding of the alkylated agent

(at least partially). These results confirm that glutathione does not bind covalently on the protein (as shown above by ITC and mass spectrometry data) and

suggest that glutathione fits into the PcEF1B γ structure, in turn hiding the cysteines (Fig. 3B).

The PcEF1B γ amino acid sequence exhibits seven tryptophan residues leading to intrinsic fluorescence of the protein with a maximum of the emission spectrum at 350 nm (excitation at 290 nm) (Fig. 4A). Adding GSSG to native PcEF1B γ led to a strong decrease (around 50%) of the fluorescence signal, while GSH had no effect on protein fluorescence. Accordingly, analysis of circular dichroism (CD) spectra showed that the binding of glutathione, particularly GSSG, modified the secondary structure of the protein by decreasing by 4% the α -helices content as estimated by CDNN spectra deconvolution (Fig. 4B). Taken together, these results showed that the binding of GSSG led to conformational changes of PcEF1B γ . Moreover, GSSG binding onto PcEF1B γ led to an increased stability of the protein as revealed by thermal shift assays (Fig. 4C). This method is based on the binding of a fluorochrome onto hydrophobic patches of a protein upon heat denaturation. It allows determining the denaturation temperature (T_d) and thus the stability of the protein. In the absence of GSSG, the T_d of PcEF1B γ was 52 °C and shifted to 54 °C and to 57 °C in the presence of 500 μ M and 2 mM GSSG, respectively, showing that GSSG stabilized the protein. It is noticeable that an additional fluorescence change occurred at around 35 °C, suggesting that a first conformational modification of the protein occurred at this temperature. This may be due to putative heat lability of the protein as shown for the recombinant rice eEF1B γ , which loses half of its activity at 34 °C [26].

It has been shown that the eEF1 γ subunit is anchored in the membrane via its C terminus and can interact with the other subunits of the EF1B complex by using its glutathione transferase-like N terminus domain [2,4]. Since we demonstrated that GSSG induces conformational changes in PcEF1B γ , it is likely that this could alter its interaction with the other subunits in conditions of oxidative stress where the cellular GSSG concentration is high.

GSSG controls the physical interaction between PcUre2pB1 and PcEF1B γ *in vitro*

The property to bind GSSG more efficiently than GSH has been already shown for GSTs from the Ure2p class in *P. chrysosporium* [25,30]. The Ure2p class is split into two subclasses Ure2pA and Ure2pB. Proteins from both subclasses exhibit similar 3D structure and share specific features as high affinity for noncovalent GSSG and ability to interact with proteins [25]. While Ure2pA isoforms are fungal-specific, highly duplicated within fungal genomes, and display the classical glutathione transferase activity, Ure2pBs are present in fungi and bacterial genomes (also named GST Nu) and the proteins display the opposite activity, that is, deglutathionylation activity. PcUre2pB1 is able to interact with proteins and to remove covalently bound glutathione from PcGSTO3, a GST from the Omega class suggesting a role in redox regulation of proteins [30]. To check whether PcUre2pB1 could have a deglutathionylation activity onto PcEF1B γ , we have used the switchSENSE biosensor technology to test in

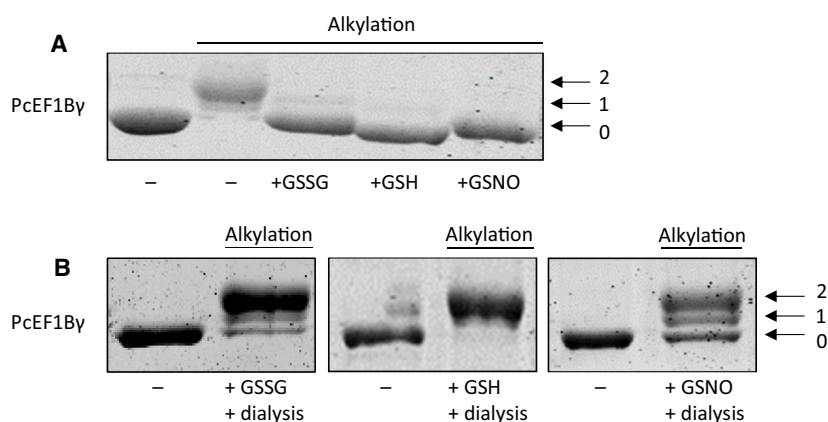


Fig. 3. Redox state of PcEF1B γ . (A) SDS/PAGE of PcEF1B γ before and after alkylation with 2 kDa mPEG-maleimide. The protein was also incubated with 2 mM of GSSG, GSH, or GSNO before alkylation. The numbers on the right correspond to the number of thiols that remained reduced and accessible upon treatment and thus were alkylated with mPEG-maleimide. (B) SDS/PAGE gel of PcEF1B γ in the presence of 2 mM of GSSG, GSH, or GSNO. In this test, a step of dialysis (Amicon Ultra centrifugal filter 10K; Millipore) has been performed after incubation with glutathione and before alkylation ($n = 3$).

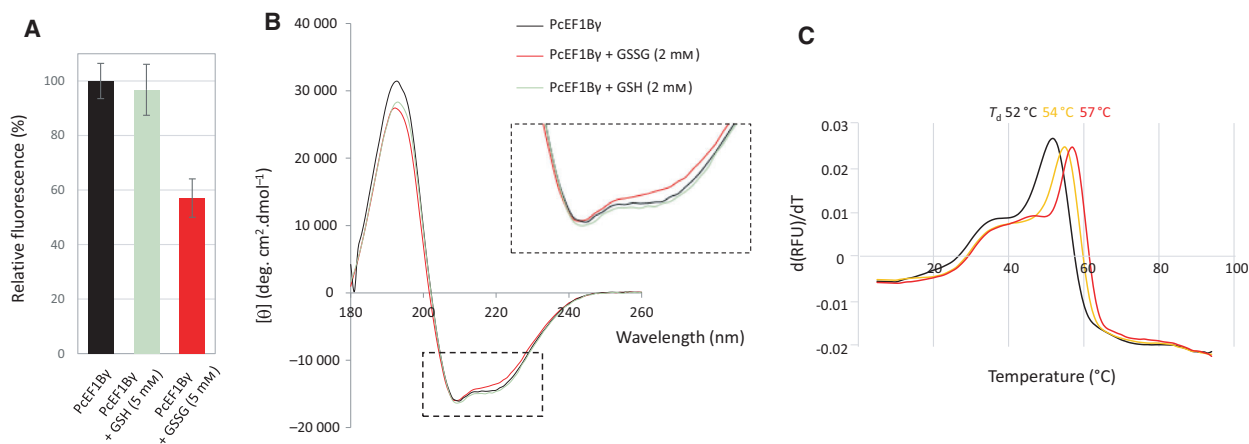


Fig. 4. Conformational modifications of PcEF1B γ induced by glutathione binding. (A) Tryptophan fluorescence modification of PcEF1B γ in the presence of GSSG. The results are expressed as a percentage, considering Apo-PcEF1B γ as the reference (100% of fluorescence) ($n = 3$). Errors bars represent standard deviation. (B) CD spectra of glutathione dependent conformational changes of PcEF1B γ . A zoom highlights the zone of interest, $[\theta]$: mean residue ellipticity. The analysis was done in duplicates with two independent protein preparations. (C) Thermal shift assay. The denaturation temperature (T_d) is reported for each condition ($n = 3$).

real time the interaction between PcEF1B γ and PcUre2pB1, with or without GSSG (Fig. 5C, kinetics raw data are provided in Fig. 6).

Apo-PcUre2pB1 (i.e., without any glutathione) was used as the ligand. Its ability to bind GSSG was first checked (Test 1). As expected, a strong interaction between Apo-PcUre2pB1 and GSSG was highlighted ($K_d = 50$ nM). The GSSG molecule was readily caught by the protein ($k_{on} = 9.54 \times 10^3$ M $^{-1}$.s $^{-1}$) and released relatively slowly in the buffer flow ($k_{off} = 0.48 \times 10^{-3}$ s $^{-1}$). The binding of GSSG onto Apo-PcUre2pB1 significantly increased the hydrodynamic diameter of the protein as determined from the time-resolved dynamics measurements, suggesting a conformational change with an expanded structure ($D_H = 4.28 \pm 0.05$ nm for the apoform and 4.47 ± 0.03 nm for the PcUre2pB1_GSSG complex; Fig. 7). Proteins are generally considered as spherical particles in which volumes were determined from the D_H values. The binding of GSSG onto PcUre2pB1 increased by 1.14-fold the apparent size of the protein (Fig. 7).

The interaction between PcUre2pB1 and PcEF1B γ was then investigated. No interaction was detected between the proteins in the absence of glutathione (Test 2). By contrast, using PcEF1B γ _GSSG as analyte (Test 3) allowed detection of association between the proteins with a good affinity ($K_d = 2.53$ μ M). In test 4, PcUre2pB1 was first saturated with GSSG before testing its association with Apo-PcEF1B γ . Under these experimental conditions, the affinity between the two proteins was better than the one measured for test 3 ($K_d = 0.77$ μ M) and the association and dissociation

rates were faster ($k_{on} = 7.94 \times 10^3$ M $^{-1}$.s $^{-1}$ and $k_{off} = 6.09 \times 10^{-3}$ s $^{-1}$). This means that PcEF1B γ efficiently recognized the particular folding of the PcUre2pB1_GSSG complex and that the interaction between the two proteins in the presence of GSSG is transient, in agreement with a putative transfer of GSSG between both proteins. In comparison with test 4, the presence of GSSG within PcEF1B γ (Test 5) decreased the association rate of the interaction between PcEF1B γ and PcUre2pB1_GSSG, but was close to that determined in test 3 ($k_{on} = 0.59$ vs. 0.58 M $^{-1}$.s $^{-1}$), where PcUre2pB1 was free of GSSG. On the contrary, the dissociation rate was slower in test 5 than in test 3, probably due to the proper conformation of PcUre2pB1 previously adopted in the presence of bound GSSG (in test 5). Since we showed above that conformational changes occurred for PcEF1B γ in presence of GSSG, it is likely that this folding modification altered the interaction between both proteins.

In test 6, the PcEF1B γ _GST domain was used as an analyte with PcUre2pB1-GSSG as ligand. The interaction was very strong ($K_d = 2.95$ nM). The association occurred very fast ($k_{on} = 76.5 \times 10^3$ M $^{-1}$.s $^{-1}$), whereas the dissociation was relatively slow ($k_{off} = 0.23 \times 10^{-3}$ s $^{-1}$), suggesting that the complex formed by PcUre2pB1-GSSG and the GST domain of PcEF1B γ was more stable than the one with the full-length PcEF1B γ . It is worthy to note that the PcEF1B γ _GST domain recognized PcUre2pB1 without any addition of GSSG, with an affinity 250 times lower than in presence of GSSG, but that remained good ($K_d = 0.76$ μ M; Test 7). Since we have detected

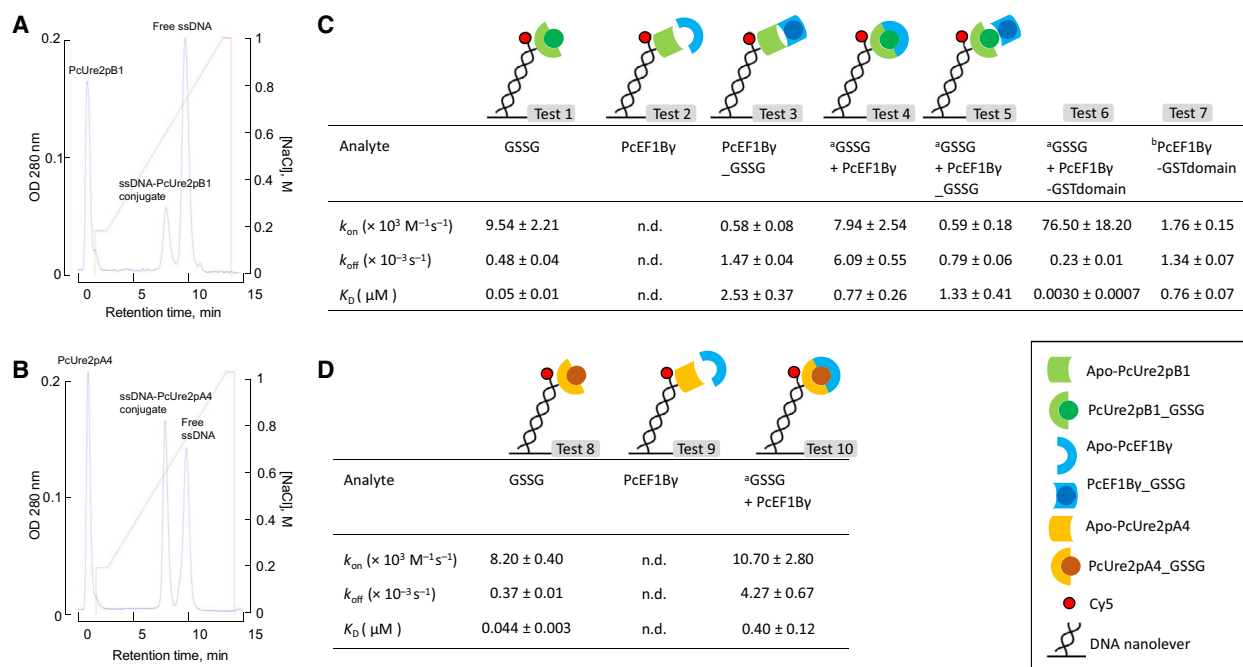


Fig. 5. Real-time switchSENSE analysis of molecular interactions. (A, B) Anion-exchange fast protein liquid chromatography of the 48-mer ssDNA- PcUre2pB1 and PcUre2pA4 conjugates performed onto an ÄKTA-Start™ system. The protein fraction that did not react was eluted in the void volume, whereas the excess of ssDNA was eluted at the end of the 0.2–1 M NaCl linear gradient performed in 50 mM sodium phosphate buffer, pH 7.2, at flow rate of 1 mL·min⁻¹ (injection of 150 μ L of reaction volume). The fraction of conjugate eluted at *ca.* 8 min for both PcUre2pB1 and PcUre2pA4 was collected and concentrated to *ca.* 35 μ L prior to buffer exchange as explained in the [Methods](#) section. (C) The Apo-PcUre2pB1 was immobilized on DNA nanolevers and tested with various analytes. ^aPcUre2pB1 was previously loaded with GSSG as analyte, rinsed, and then tested for the second analyte PcEF1B γ , PcEF1B γ _GSSG, or PcEF1B γ _GST domain. ^bGSH was detected within the GST domain by mass spectrometry. n.d., not determined (no interaction). (D) The Apo-PcUre2pA4 was immobilized on DNA nanolevers and tested with various analytes. All kinetic curves were analyzed by nonlinear fitting of single-exponential functions with the SWITCHANALYSIS[®] software. Each kinetic experiment was performed twice with different sample preparations.

the presence of GSH by mass spectrometry within the PcEF1B γ _GST domain sample, it is likely that it could have favored the interaction.

Taken together, these results showed that PcUre2pB1 and PcEF1B γ physically interact in the presence of GSSG. This interaction occurred at the N-terminal part of PcEF1B γ and the specific conformations of PcUre2pB1_GSSG and Apo-PcEF1B γ are optimal for the complex formation.

Since all the members of the Ure2p class that we have previously characterized share the same ability to bind GSSG [25], we have tested the interaction between PcEF1B γ and another Ure2p from *P. chrysosporium*, PcUre2pA4 (Fig. 5D). Similarly to PcUre2pB1 and in accordance with our previous studies, PcUre2pA4 exhibited a high affinity for GSSG ($K_D = 44$ nM). The binding of GSSG led to a conformational change of the protein increasing its hydrodynamic diameter from 5.89 to 6.41 nm (Fig. 7). PcUre2pA4 and PcEF1B γ physically

interacted in the presence of GSSG previously bound to PcUre2pA4, suggesting that the interaction between PcEF1B γ and Ure2p is not protein-dependent but is rather linked to the ability of proteins from the Ure2p class to bind GSSG. The 3D structures of both PcUre2pB1 and PcUre2pA4 have been solved and revealed two binding sites for glutathione [25,30]. The binding site of the first glutathione moiety (GS-1) is the G-site of GSTs, while the second moiety (GS-2) is more solvent-exposed and stabilized by the side chain of a conserved arginine from the opposite subunit. This exposed GS-2 could thus be recognized by PcEF1B γ . On the basis that GST can accommodate many structurally different substituents linked to GSH, it has already been suggested that they can selectively interact with certain S-glutathionylated proteins through the recognition of a GSH moiety that is covalently bound onto cysteines; however, no clear evidence has been provided [31]. In this study, we report for the first time GSSG-dependent

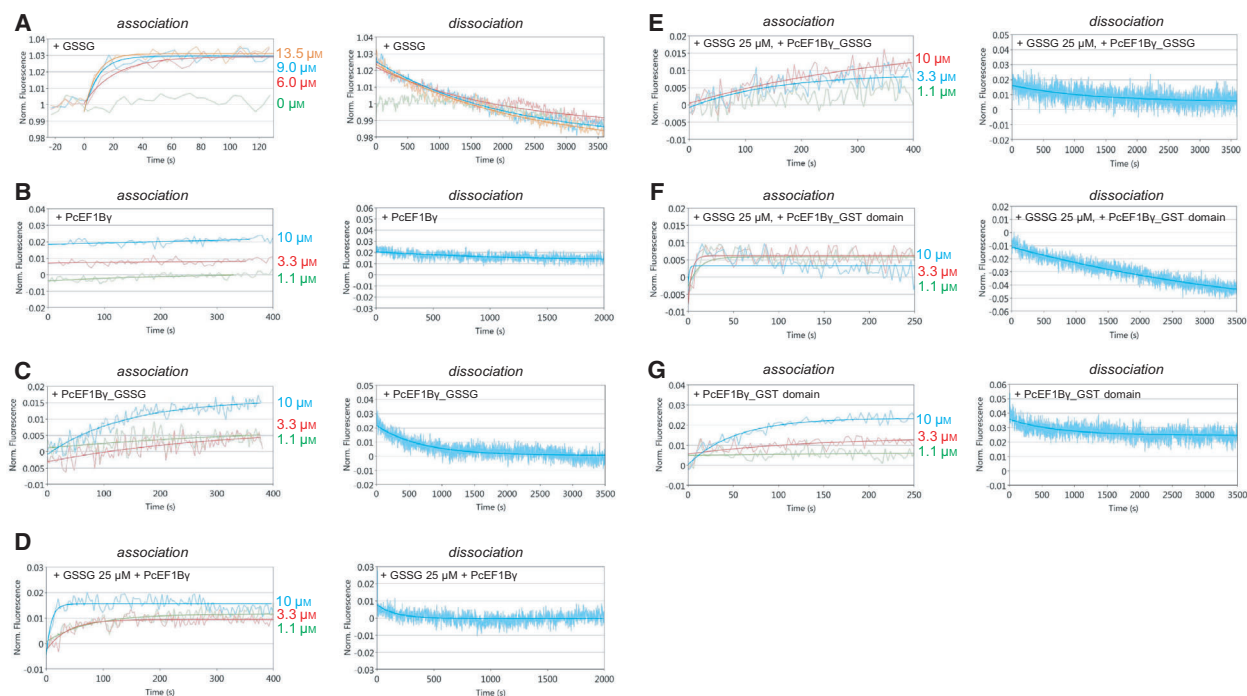


Fig. 6. Kinetics analysis of PcUre2pB1 interacting with GSSG (A), PcEF1B γ (B–E), and PcEF1B γ _GST domain (F, G) by using the switchSENSE technology. The raw data are superimposed by global exponential fits for various concentrations of each analyte. A blank control performed with PE40 buffer instead of analyte was subtracted to normalize the signal, except in the case of GSSG, for which the blank (0 μ M GSSG) did not generate any significant signal. The k_{on} , k_{off} , and K_d were determined for each kinetics measurement. All kinetic curves were analyzed by nonlinear fitting of single-exponential functions with the SWITCHANALYSIS® software. Each kinetic experiment was performed twice with different sample preparations.

protein–protein interaction. Thus, we postulate that the interaction between PcUre2p and PcEF1B γ -1 could occur upon oxidative stress, when the intracellular concentration of oxidized glutathione is high. This could be a way to couple the redox balance of the cell to stress response regulation by modifying PcEF1B γ activity.

Conclusion

Both the conformational changes of PcEF1B γ due to GSSG binding and its ability to interact with Ure2p proteins are of particular importance since eEF1B γ interacts with other components of the elongation complex through its N-terminal domain. In human, the presence of glutathione does not affect the capacity of NT-heEF1 γ to form a complex with NT-heEF1 β [2]. In ScTEF3, glutathione fits into the structure close to a loop located between β 2 and α 2. It has been first suggested that this loop could be important for the interaction between eEF1B γ and eEF1B β [27]. However, the 3D structure of the heEF1 β and heEF1 γ GST-like domains (<https://doi.org/10.2210/pdb5DQS/pdb>) reveals that this loop is not directly involved in the interaction between both proteins. Rather, since it is solvent-exposed, it could add

flexibility to the region and be part of eEF1B γ active site. The next step will be to check whether the complex formation with Ure2p in the presence of GSSG could be a way to couple the redox balance of the cell to stress response regulation by modifying PcEF1B γ interaction with the other components of the elongation factor complex or by altering other putative functions of PcEF1B γ . In microbes, but also in other organisms especially in human, understanding the regulation of eEF1B γ is of great importance. Indeed, eEF1B γ also possesses non-canonical functions related to crucial cellular processes that are affected in cancer cells or neurodegenerative disorders as micro-RNA turnover, splicing and stability of mRNA, cell cycle regulation, or cytoskeleton integrity [32].

Methods

Production and purification of recombinant PcEF1B γ , PcEF1B γ _GST domain, PcUre2pB1, and PcUre2pA4

The sequence encoding the full-length PcEF1B γ (ProtID 2934909 from the Joint Genome Institute JGI v2.2) was

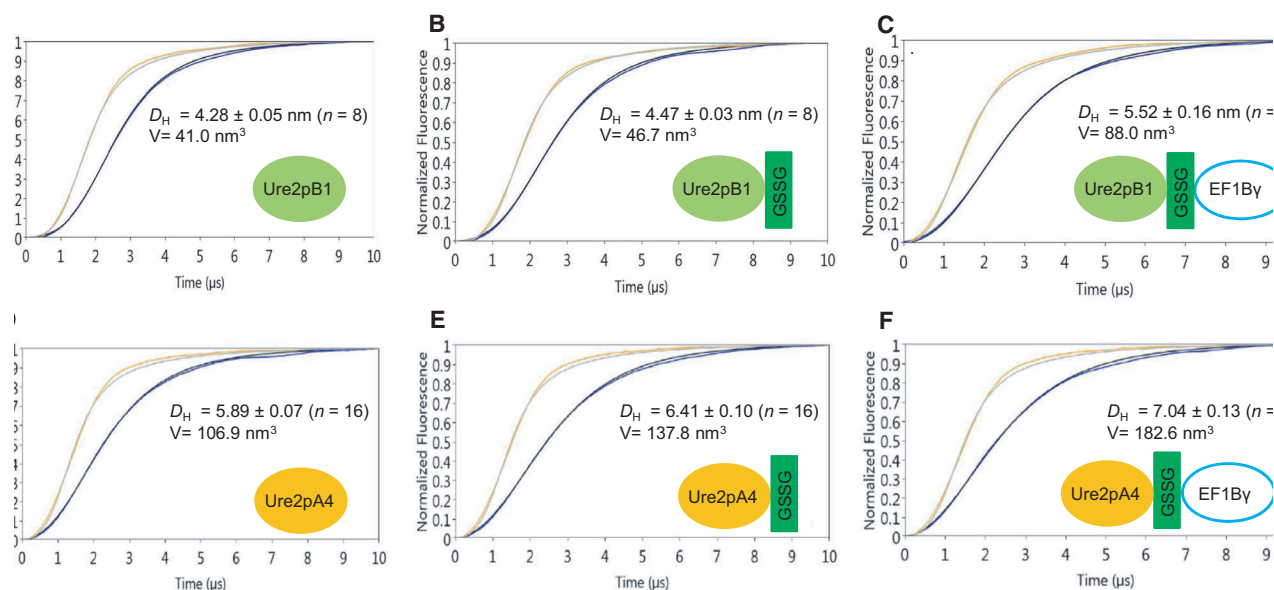


Fig. 7. Determination of the hydrodynamic diameter (D_H) and calculated volumes (V) of PcUre2pB1 and PcUre2pA4 attached to the nanolever's distal end, in the absence of analyte (A, D), in the presence of GSSG (B, E), and in the presence of PcEF1B γ _GSSG (C, F). The fluorescence response was measured by time-correlated single-photon counting during the first 10 μs of upward switching. Orange and gray curves correspond to the raw data and their fitting in the case of the reference, respectively, and the blue and black curves to the raw data and their fitting in the case of the samples, respectively. $n = 8$ for all measurements except for Ure2pA4 and Ure2pA4_GSSG ($n = 16$).

amplified from cDNAs of *P. chrysosporium* RP-78 strain using the Herculase[®] II Fusion Enzyme (Agilent Technologies, Santa Clara, CA, USA) with the 5'CCCCCATATGTCCTCGGTACGCTC3' and 5'CCCCGCGCCGCTTAGTTCCTTGCCATCGACCA3' primers and cloned into the NdeI and NotI restriction sites of pET-26b plasmid (Novagen, Madison, WI, USA), without any tag. The GST domain of PcEF1B γ was only obtained using a His-tag-based purification method. The sequence was cloned into pET-26b plasmid (Novagen) between NdeI and NotI restriction sites in frame with a His-tag at the C-terminal end. The primers 5'CCCCCATATGTCCTCGGTACGCTC3' and 5'CCCCGCGCCGCTTAGTTCCTTGCCATCGACCA3' were used. The proteins were expressed in *Escherichia coli* Rosetta2 (DE3) pLysS strain (Novagen) after adding 100 mM isopropyl β -D-thiogalactopyranoside for 3 h at 37 °C. The cultures were then centrifuged for 30 min at 4400 g . The pellets were resuspended in 15 mL of lysis buffer (30 mM Tris-HCl, pH 8.0). Cell lysis was performed on ice by sonication. Polyethylenimine at 0.05% was added to the sample to precipitate DNA, and the soluble and insoluble fractions were separated by centrifugation for 30 min at 27 000 g . For the full-length PcEF1B γ , the soluble part was fractionated by precipitating part of the proteins with 40% ammonium sulfate. After centrifugation, the supernatant containing PcEF1B γ was subjected to a combination of phenyl-Sepharose, DEAE-cellulose, and size exclusion chromatographies.

For the PcEF1B γ _GST domain, 10 mM imidazole was added in the soluble fraction before loading onto a Ni-NTA (Ni²⁺-nitrilotriacetate)-agarose resin. After a washing step with lysis buffer supplemented with 20 mM imidazole, the proteins were eluted using an imidazole gradient from 20 to 500 mM. The fractions of interest were pooled, dialyzed, concentrated by ultrafiltration under nitrogen pressure (Amicon YM10 membrane; Merck Millipore, Darmstadt, Germany), and finally stored in 30 mM Tris-HCl, pH 8.0 at -20 °C. PcUre2pB1 and PcUre2pA4 were produced and purified as previously described [25,30].

Oligomerization state determination by size exclusion chromatography-multi-angle light scattering

An ÄKTA-Purifier unit and a Superdex 200 10/300 column (GE Healthcare, Chicago, IL, USA) were used. This FPLC system was coupled online with a UV 900 detector (GE Healthcare), a multi-angle light scattering detector (miniDAWN TREOS II; Wyatt Technology, Santa Barbara, CA, USA), and a differential refractometer (Optilab T-rEX; Wyatt Technology). Runs were carried out with 600 μg of pure PcEF1B γ or PcEF1B γ _GST domain in 300 μL final volume of 30 mM Tris-HCl buffer, pH 8.0, containing 200 mM NaCl, and 0.02% sodium azide at 20 °C. The flow rate was 0.5 mL \cdot min⁻¹. Data were analyzed using the manufacturer supplied software (ASTRA

6.1; Wyatt Technology) to determine the size of oligomers.

Enzymatic activity measurement

The activity of PcEF1B γ and PcEF1B γ _GST domain was assayed using the classical chlorodinitrobenzene (CDNB) substrate used for GST transferase activity measurement *in vitro*. The GST activity is determined by measuring the rate of produced conjugation between reduced glutathione and CDNB forming a CDNB-SG conjugate, which is proportional to the increase in absorbance at 340 nm over time ($\Delta\text{OD}_{340} \text{ nm}\cdot\text{min}^{-1}$). The reactions were performed in triplicate in 100 mM phosphate buffer, pH 6.5, in the presence of 2 mM GSH. The K_M value for GSH and CDNB was determined using a GSH concentration ranging from 0 to 10 mM in the presence of 2 mM of CDNB and a CDNB concentration ranging from 0 to 10 mM in the presence of 2 mM GSH. The apparent k_{cat} value for CDNB was determined in the presence of 2 mM GSH using a CDNB concentration ranging from 0 to 10 mM. The reactions were started by addition of the purified enzyme and monitored with a Cary 50 UV-visible spectrophotometer (Agilent Technologies). The catalytic parameters were calculated using GRAPHPAD software (GraphPad Software, San Diego, CA, USA).

Isothermal titration calorimetry

The ITC measurements were performed using a MicroCal iTC200 calorimeter (Malvern Instruments, Malvern, UK), under constant stirring at 1000 r.p.m. and 25 °C and a reference power of 10 $\mu\text{cal}\cdot\text{s}^{-1}$. PcEF1B γ and PcEF1B γ _GST domain (25 μM) were titrated by GSH or GSSG (1 mM) in 30 mM Tris-HCl buffer, pH 8.0. Aliquots of the titrant were successively injected into the sample cell at 120-s intervals. A total of 25 injections split in three sets (successive injection volumes of 0.5, 1.0, and 2.0 μL) of GSH or GSSG were performed. The integrated heat data were fit to the one-set-of-sites model in the ORIGIN software (Malvern Instruments, Malvern, UK). The dilution heat of the titrant (i.e., glutathione injected into protein-free buffer) was subtracted from the sample data. The experiments were carried out twice with different sample preparations.

Alkylation tests

The redox state of PcEF1B γ was checked with SDS/PAGE gels using the alkylation agent mPEG-maleimide that specifically binds free thiols. Four microgrammes of PcEF1B γ were incubated with 2 mM GSSG, GSH, or GSNO for 3 h at 25 °C in Tris 30 mM pH 8.0 and treated with maleimide polyethylene glycol of 2 kDa (2 kDa mPEG-maleimide) as described previously [33]. In order to remove glutathione

from PcEF1B γ , a step of dialysis (Amicon Ultra centrifugal filter 10K; Merck Millipore) was added after incubation with GSSG, GSH, or GSNO and before alkylation.

Tryptophan fluorescence

The fluorescence of PcEF1B γ were recorded with a spectrofluorometer (Cary Eclipse; Agilent Technologies) in 100 mM Tris-HCl buffer, pH 8.0 buffer at a protein concentration of 0.7 μM . After excitation at 290 nm, the protein displayed an emission spectrum with a maximum at 350 nm characteristic of a fluorescence signal strongly dominated by tryptophan. Spectra were recorded for PcEF1B γ as purified (i.e., without any glutathione) and after addition of 5 mM of either GSSG or GSH.

Thermal shift assays

The experiments were performed in 96-well microplates (Harshell, Biorad, Hercules, CA, USA) using a real-time PCR detection system (CFX 96 touch; BioRad). The assays were performed in a total volume of 25 μL per well containing 30 mM Tris-HCl buffer, pH 8.0 buffer, in the presence of 500 μM or 2 mM GSSG, 10 μM protein, and 2 μL of SYPRO orange (previously diluted 63-fold in ultrapure water). The plate was centrifuged for 30 s at 4000 *g*. Fluorescence was measured (excitation wavelength: 485 nm; emission wavelength: 530 nm) every minute starting from 3 min at 5 °C while increasing temperature from 5 °C to 95 °C with a step of 1 °C $\cdot\text{min}^{-1}$. The denaturation temperature (T_d) corresponds to the temperature where 50% of the total fluorescence was measured. The T_d value was determined by using the nonlinear regression Boltzmann sigmoidal model in GRAPHPAD PRISM 6 software.

Circular dichroism

The CD spectra of PcEF1B γ (20 μM) were obtained in 20 mM phosphate buffer pH 8.0 at 25 °C in a quartz cuvette (1 mm path length) from 180 to 250 nm with a bandwidth of 1 nm using a Chirascan Plus spectropolarimeter (Applied Photophysics Ltd, Leatherhead, UK). Apo-PcEF1B γ was tested with or without 2 mM GSSG or GSH. The mean residue ellipticity [h]MR was calculated using PRO-DATA VIEWER (Applied Photophysics) software and expressed in $\text{deg}\cdot\text{cm}^2\cdot\text{dmol}^{-1}$ per residue.

Time-resolved molecular dynamics measurement

Real-time analyses of biomolecular interactions, between PcEF1B γ or PcEF1B γ _GST domain and two glutathione transferases of the Ure2p class: PcUre2pB1 and PcUre2pA4, were investigated.

Preparation and immobilization of the ligands

Apo-PcUre2pB1 and Apo-PcUre2pA4 were used as ligands. To get the apoform of the proteins, they were DTT-reduced (3 h at room temperature, 10 mM DTT in 30 mM Tris-HCl buffer, pH 8.0) and dialyzed. Indeed, even if GSSG is not covalently bound onto PcUre2ps, a DTT treatment leading to the reduction of GSSG into GSH allows removing glutathione from the proteins after dialysis because the affinity of the PcUre2ps for GSH is much lower than for GSSG [30]. PcUre2pB1 and PcUre2pA4 were immobilized on an electro-switchable DNA chip MPC-48-2-R1-S placed into a biosensor analyzer switchSENSE[®] DRX (Dynamic Biosensors GmbH, Planegg, Germany) according to Ref. [34]. Covalent conjugates between the ligands and a 48mer ssDNA were prepared with the amine coupling kit supplied by Dynamic Biosensors and purified by anion-exchange chromatography onto an ÄKTA-Start[™] system (GE Healthcare). The purified conjugates were then diluted at 200 nM in 10 mM NaH₂PO₄/Na₂HPO₄ buffer, pH 7.4, containing 40 mM NaCl, 50 μ M EDTA, 50 μ M EGTA, and 0.05% Tween 20 (PE40 buffer). A volume of 25 μ L of conjugate was injected into the chip to form fluorescent PcUre2pB1-dsDNA and PcUre2pA4-dsDNA nanolevers.

Fluorescence static measurements

Various analytes were tested for interaction with the PcUre2ps ligands: GSSG, Apo-PcEF1B γ , PcEF1B γ _GSSG, and PcEF1B γ _GST domain. PcEF1B γ was purified under its apoform. The glutathionylated form of PcEF1B γ was obtained after incubation with 2 mM GSSG at room temperature for 3 h in 30 mM Tris-HCl, pH 8.0. The protein was then dialyzed twice in 30 mM Tris-HCl buffer pH 8.0 in a 1 : 100 sample/buffer ratio during 2 h and overnight in fresh buffer to remove excess of GSSG. To perform fluorescence static measurements (fluorescence proximity sensing responds to changes to the molecular environment upon analyte binding), serial dilutions of each analyte were prepared from samples at 10 μ M in PE40. For experiments with PcEF1B γ , the PE40 buffer also contained salmon sperm DNA at 100 μ g·mL⁻¹ (Eurobio Ingen, Les Ulis, France) to prevent unspecific binding of the protein onto the DNA nanolevers. The diluted protein analytes were injected into the microfluidic at a flow rate of 5 μ L·min⁻¹ for 5 min (at 25 °C), and PE40 was then injected at 30 μ L·min⁻¹ for 60 min to determine the affinity constant $K_d = k_{\text{off}}/k_{\text{on}}$ of each complex from the association (k_{on}) and dissociation (k_{off}) kinetics constants. For experiments performed in the presence of GSSG using the 'sandwich' format available in the SWITCHBUILD[®] software (Dynamic Biosensors GmbH, Planegg, Germany), GSSG at 25 μ M in PE40 was injected at 50 μ L·min⁻¹ for 15 min prior to the injection of

PcEF1B γ or PcEF1B γ _GST domain. When GSSG was used as the only analyte, it was injected at 50 μ L·min⁻¹ for 2 min, and then, the PE40 buffer was injected at 50 μ L·min⁻¹ for 60 min. A blank control was systematically performed with PE40 instead of analyte and subtracted to normalize the signal.

Molecular dynamics measurements

The hydrodynamic diameters (D_H) of the ligands (PcUre2pB1 and PcUre2pA4) were determined with the Lollipop mathematical model. After association, the flow of the analyte solution was stopped, and the hydrodynamic diameter of the complex was determined from fluorescence relaxation measurements of the switching nanolevers. All kinetic curves were analyzed by nonlinear fitting of single-exponential functions with the SWITCHANALYSIS[®] software (Dynamic Biosensors GmbH). Each kinetic experiment was performed twice with different sample preparations. The D_H values were the mean of 8 or 16 measurements depending on the sample. Knowing the mean D_H values, the volumes of the proteins and complexes were calculated as volumes of spherical particles.

Acknowledgements

This work was supported by the French National Research Agency (ANR) as part of the 'Investissements d'Avenir' programme (ANR-11-LABX-0002-01, Lab of Excellence ARBRE). Biomolecular interactions were investigated with the ITC and switchSENSE technologies available on the ASIA platform (Université de Lorraine-INRA; <https://a2f.univ-lorraine.fr/asia/>). We thank Alexandre Kriznik for CD data (UMR7365 UL/CNRS IMoPA, Nancy, France) and Tiphaine Dhalleine and Arnaud Hecker (UMR1136 INRAE/UL IAM, Nancy, France) for technical assistance with chromatographic methods. We thank JP Jacquot for reviewing and improving the manuscript.

Conflict of interest

The authors declare no conflict of interest.

Author contributions

EG and MM-R conceived the project and designed experiments. RB, RS and J-MG performed the experiments. MM-R and J-MG wrote the manuscript. RB, EG, J-MG, and MM-R edited the manuscript. RB, J-MG, and MM-R conducted data analysis. All authors have read and approved the final manuscript.

References

- Sasikumar AN, Perez WB & Kinzy TG (2012) The many roles of the eukaryotic elongation factor 1 complex. *Wiley Interdiscip Rev RNA* **3**, 543–555.
- Achilonu I, Elebo N, Hlabano B, Owen GR, Papathanasopoulos M & Dirr HW (2018) An update on the biophysical character of the human eukaryotic elongation factor 1 beta: perspectives from interaction with elongation factor 1 gamma. *J Mol Recognit* **31**, e2708.
- Sanders J, Brandsma M, Janssen GM, Dijk J & Möller W (1996) Immunofluorescence studies of human fibroblasts demonstrate the presence of the complex of elongation factor-1 beta gamma delta in the endoplasmic reticulum. *J Cell Sci* **109**, 1113–1117.
- Trosiuk TV, Shalak VF, Szczepanowski RH, Negrutskii BS & El'skaya AV (2016) A non-catalytic N-terminal domain negatively influences the nucleotide exchange activity of translation elongation factor 1B α . *FEBS J* **283**, 484–497.
- Liu D, Sheng C, Gao S, Jiang W, Li J, Yao C, Chen H, Wu J, Chen S & Huang W (2014) eEF1B γ is a positive regulator of NF- κ B signaling pathway. *Biochem Biophys Res Commun* **446**, 523–528.
- Kim S, Kellner J, Lee CH & Coulombe PA (2007) Interaction between the keratin cytoskeleton and eEF1B gamma affects protein synthesis in epithelial cells. *Nat Struct Mol Biol* **14**, 982–983.
- Corbi N, Batassa EM, Pisani C, Onori A, Di Certo MG, Strimpakos G, Fanciulli M, Mattei E & Passananti C (2010) The eEF1 gamma subunit contacts RNA polymerase II and binds vimentin promoter region. *PLoS One* **5**, e14481.
- Mimori K, Mori M, Tanaka S, Akiyoshi T & Sugimachi K (1995) The overexpression of elongation factor 1 gamma mRNA in gastric carcinoma. *Cancer* **75**, 1446–1449.
- Mimori K, Mori M, Inoue H, Ueo H, Mafune K, Akiyoshi T & Sugimachi K (1996) Elongation factor 1 gamma mRNA expression in oesophageal carcinoma. *Gut* **38**, 66–70.
- Le Sourd F, Boulben S, Le Bouffant R, Cormier P, Morales J, Belle R & Mulner-Lorillon O (2006) eEF1B: at the dawn of the 21st century. *Biochim Biophys Acta* **1759**, 13–31.
- Pisani C, Onori A, Gabanella F, Delle Monache F, Borreca A, Ammassari-Teule M, Fanciulli M, Di Certo MG, Passananti C & Corbi N (2016) eEF1B γ binds the Che-1 and TP53 gene promoters and their transcripts. *J Exp Clin Cancer Res* **35**, 146.
- Valouev IA, Fominov GV, Sokolova EE, Smirnov VN & Ter-Avanesyan MD (2009) Elongation factor eEF1B modulates functions of the release factors eRF1 and eRF3 and the efficiency of translation termination in yeast. *BMC Mol Biol* **10**, 60.
- Olarewaju O, Ortiz PA, Chowdhury WQ, Chatterjee I & Kinzy TG (2004) The translation elongation factor eEF1B plays a role in the oxidative stress response pathway. *RNA Biol* **1**, 89–94.
- Esposito AM & Kinzy TG (2010) The eukaryotic translation elongation factor 1B gamma has a non-guanine nucleotide exchange factor role in protein metabolism. *J Biol Chem* **285**, 37995–38004.
- Thuillier A, Chibani K, Belli G, Herrero E, Dumarçay S, Gérardin P, Kohler A, Deroy A, Dhalleine T, Bchini R *et al.* (2014) Transcriptomic responses of *Phanerochaete chrysosporium* to oak acetonic extracts: focus on a new glutathione transferase. *Appl Environ Microbiol* **80**, 6316–6327.
- McIlwain CC, Townsend DM & Tew KD (2006) Glutathione S-transferase polymorphisms: cancer incidence and therapy. *Oncogene* **25**, 1639–1648.
- Zhao Y, Dong W, Zhu Y, Allan AC, Lin-Wang K & Xu C (2019) PpGST1, an anthocyanin-related glutathione S-transferase gene, is essential for fruit coloration in peach. *Plant Biotechnol J* **18**, 1284–1295.
- Mathieu Y, Prosper P, Favier F, Harvengt L, Didierjean C, Jacquot JP, Morel-Rouhier M & Gelhaye E (2013) Diversification of fungal specific class a glutathione transferases in saprotrophic fungi. *PLoS One* **8**, e80298.
- Parker LJ, Bocedi A, Ascher DB, Aitken JB, Harris HH, Lo Bello M, Ricci G, Morton CJ & Parker MW (2017) Glutathione transferase P1–1 as an arsenic drug-sequestering enzyme. *Protein Sci* **26**, 317–326.
- Litwack G, Ketterer B & Arias IM (1971) Ligandin: a hepatic protein which binds steroids, bilirubin, carcinogens and a number of exogenous organic anions. *Nature* **234**, 466–467.
- Brock J, Board PG & Oakley AJ (2013) Structural insights into omega-class glutathione transferases: a snapshot of enzyme reduction and identification of a non-catalytic ligandin site. *PLoS One* **8**, e60324.
- McGoldrick S, O'Sullivan SM & Sheehan D (2005) Glutathione transferase-like proteins encoded in genomes of yeasts and fungi: insights into evolution of a multifunctional protein superfamily. *FEMS Microbiol Lett* **242**, 1–12.
- Morel M, Ngadin AA, Droux M, Jacquot J-P & Gelhaye E (2009) The fungal glutathione S-transferase system. Evidence of new classes in the wood-degrading basidiomycete *Phanerochaete chrysosporium*. *Cell Mol Life Sci* **66**, 3711–3725.
- Achilonu I, Siganunu TP & Dirr HW (2014) Purification and characterisation of recombinant human eukaryotic elongation factor 1 gamma. *Protein Expr Purif* **99**, 70–77.

- 25 Roret T, Thuillier A, Favier F, Gelhaye E, Didierjean C & Morel-Rouhier M (2015) Evolutionary divergence of Ure2pA glutathione transferases in wood degrading fungi. *Fungal Genet Biol* **83**, 103–112.
- 26 Kobayashi S, Kidou S & Ejiri S (2001) Detection and characterization of glutathione S-transferase activity in rice EF-1betabeta'gamma and EF-1gamma expressed in *Escherichia coli*. *Biochem Biophys Res Commun* **288**, 509–514.
- 27 Jeppesen MG, Ortiz P, Shepard W, Kinzy TG, Nyborg J & Andersen GR (2003) The crystal structure of the glutathione S-transferase-like domain of elongation factor 1Bgamma from *Saccharomyces cerevisiae*. *J Biol Chem* **278**, 47190–47198.
- 28 Vickers TJ & Fairlamb AH (2004) Trypanothione S-transferase activity in a trypanosomatid ribosomal elongation factor 1B. *J Biol Chem* **279**, 27246–27256.
- 29 Tshabalala TN, Tomescu MS, Prior A, Balakrishnan V, Sayed Y, Dirr HW & Achilonu I (2016) Energetics of glutathione binding to human eukaryotic elongation factor 1 gamma: isothermal titration calorimetry and molecular dynamics studies. *Protein J* **35**, 448–458.
- 30 Thuillier A, Roret T, Favier F, Gelhaye E, Jacquot JP, Didierjean C & Morel-Rouhier M (2013) Atypical features of a Ure2p glutathione transferase from *Phanerochaete chrysosporium*. *FEBS Lett* **587**, 2125–2130.
- 31 Listowsky I (2005) Proposed intracellular regulatory functions of glutathione transferases by recognition and binding to S-glutathiolated proteins. *J Pept Res* **65**, 42–46.
- 32 Negrutskii B (2020) Non-translational connections of eEF1B in the cytoplasm and nucleus of cancer cells. *Front Mol Biosci* **7**, 56.
- 33 Zannini F, Couturier J, Keech O & Rouhier N (2017) *In vitro* alkylation methods for assessing the protein redox state. *Photorespiration* **1653**, 51–64.
- 34 Langer A, Hampe PA, Kaiser W, Knezevic J, Welte T, Villa V, Maruyama M, Svejda M, Jähner S, Fischer F *et al.* (2013) Protein analysis by time-resolved measurements with an electro-switchable DNA chip. *Nat Commun* **4**, 2099.